

Quantitative at-line monitoring of enzymatic hydrolysis using benchtop diffusion nuclear magnetic resonance spectroscopy

Evan R. McCarney¹  | Kenneth A. Kristoffersen^{2,3} | Kathryn E. Anderssen^{2,4}

¹Korimako Chemical Ltd, Wellington, New Zealand

²Nofima AS—Norwegian Institute of Food, Fisheries and Aquaculture Research, Ås, Norway

³Faculty of Chemistry, Biotechnology and Food Science, NMBU—Norwegian University of Life Sciences, Ås, Norway

⁴Department of seafood industry, Nofima AS, Tromsø, Norway

Correspondence

Kathryn E. Anderssen, Department of seafood industry, Nofima AS, PO Box 6122, NO-9291 Tromsø, Norway.
Email: kate.anderssen@nofima.no

Funding information

Mabit, Grant/Award Number: UB0071; Novozymes

Abstract

Benchtop diffusion nuclear magnetic resonance (NMR) spectroscopy was used to perform quantitative monitoring of enzymatic hydrolysis. The study aimed to test the feasibility of the technology to characterize enzymatic hydrolysis processes in real time. Diffusion ordered spectroscopy (DOSY) was used to measure the signal intensity and apparent self-diffusion constant of solubilized protein in hydrolysate. The NMR technique was tested on an enzymatic hydrolysis reaction of red cod, a lean white fish, by the endopeptidase alcalase at 50°C. Hydrolysate samples were manually transferred from the reaction vessel to the NMR equipment. Measurement time was approximately 3 min per time point. The signal intensity from the DOSY experiment was used to measure protein concentration and the apparent self-diffusion constant was converted into an average molecular weight and an estimated degree of hydrolysis. These values were plotted as a function of time and both the rate of solubilization and the rate of protein breakdown could be calculated. In addition to being rapid and noninvasive, DOSY using benchtop NMR spectroscopy has an advantage compared with other enzymatic hydrolysis characterization methods as it gives a direct measure of average protein size; many functional properties of proteins are strongly influenced by protein size. Therefore, a method to give protein concentration and average size in real time will allow operators to more tightly control production from enzymatic hydrolysis. Although only one type of material was tested, it is anticipated that the method should be applicable to a broad variety of enzymatic hydrolysis feedstocks.

KEYWORDS

DOSY, enzymatic hydrolysis, nuclear magnetic resonance spectroscopy, process monitoring

This is an open access article under the terms of the [Creative Commons Attribution-NonCommercial-NoDerivs](https://creativecommons.org/licenses/by-nc-nd/4.0/) License, which permits use and distribution in any medium, provided the original work is properly cited, the use is non-commercial and no modifications or adaptations are made.

© 2024 The Authors. *Magnetic Resonance in Chemistry* published by John Wiley & Sons Ltd.

1 | INTRODUCTION

1.1 | Enzymatic hydrolysis of food by-products

Primary industries have an incentive to increase sustainability and decrease the burden on natural resources. Most industries produce significant waste streams that typically get diverted to low-value feed stock. In the fishing industry, low-value by-products, for example, heads, tails, or entrails, are mostly sold only to be turned into fish feed.¹ Agricultural by-products are also commonly used as livestock feed. Although, these by-products often contain valuable protein, harvesting it in an efficient manner has been challenging.² Recent advances in enzymatic hydrolysis have shown that the method can be used to break the waste products down into their primary components, such that higher value products can be manufactured from them.³⁻⁵ For example, hydrolysis of proteinaceous by-products can produce valuable functional peptides for use in the nutraceutical, pharmaceutical, and beauty industries.⁶ In order to be used in higher value products, peptides of the proper size must be produced from the by-products. Functional properties such as foaming capacity, emulsification capacity, and solubility all have a dependence on protein size.⁷ Taste is another factor, as smaller peptides are associated with bitter flavor that makes them unsuitable for use in food products.⁸ However, hydrolysis is a complicated process that is not fully understood. The products of enzymatic hydrolysis, hydrolysates, will depend on the starting materials, the enzymes used, and the reaction conditions.⁹⁻¹² A method to monitor the enzymatic hydrolysis process in real time would be valuable in order to consistently produce peptides of the desired size.

To date, it has not been possible to monitor changes in protein size during enzymatic protein hydrolysis (EPH) in real time. Most studies that follow hydrolysis reactions deactivate the hydrolytic enzymes prior to analysis. The pH-stat method is commonly used to monitor the degree of hydrolysis (*DH*) during EPH reactions. The method is based on the number of protons released during hydrolysis, which are measured by preventing pH drift by the titration of hydroxide. This is limited to small reaction sizes that can be titrated in-situ or subsamples of larger reactions that have been deactivated. Chromatography lacks the temporal resolution required for following hydrolysis reactions, is time consuming, and often requires careful calibration. This leaves a gap in direct monitoring hydrolysis on an industrial scale. Standard spectroscopy techniques like Fourier-transform infrared are currently being investigated^{13,14}; however, these methods cannot currently be

performed online and are indirect measurements that typically rely on multivariate models to predict hydrolysate progress. Multivariate models are prone to developing local calibrations that are not globally applicable. This can make them unstable when applied to highly variable materials like by-products, where the composition and ratios of different constituents will often change significantly from batch to batch.

Established methods for determining molecular weights of protein mixtures include sodium dodecyl sulfate polyacrylamide gel electrophoresis (SDS-PAGE) and size exclusion chromatography (SEC). Although SDS-PAGE is common in protein analysis, it is not frequently used in EPH analysis, where SEC is the dominant method. Infrared spectroscopy coupled with multivariate analysis has recently shown promise as a faster method for characterizing protein hydrolysates. This has been calibrated with molecular mass average measurements calculated from the SEC profiles.¹³ SEC is a chromatography method that separates proteins by hydrodynamic radius as they flow through a tortuous stationary medium. The small molecules get obstructed by beads, while the larger molecules flow around them, resulting in a chromatogram with elution times inversely correlated to hydrodynamic radius. The hydrodynamic radius of proteins and peptides is determined by molecular weight and packing efficiency, which is often influenced by hydrophobic and charged composition of macromolecules. The standard detector for SEC is a UV absorption spectrometer, which is most sensitive to the amide bond of proteins and peptides and tends to miss individual amino acids. In addition, SEC relies on a limited molecular weight range of the column and requires frequent calibration.¹⁵

Nuclear magnetic resonance (NMR) is an established method for measuring the hydrodynamic radius of proteins and peptides using pulsed field gradient methods.¹⁶ The hydrodynamic radius scales with the size and mass of the molecule. In general, the diffusion coefficient of a molecule is inversely proportional to its hydrodynamic radius. Molecules with larger hydrodynamic radii diffuse more slowly because they experience more interactions with surrounding molecules than smaller molecules, which have less resistance and can move more freely. Therefore, by using pulse field gradient methods to measure the distribution of diffusion coefficients in a solution, NMR is able to estimate molecule weights of proteins.¹⁷⁻²² It is important to note that in certain cases, the relationship between molecular diffusion and hydrodynamic radius can be more complex, in particular when considering nonspherical or complex-shaped molecules.

Recently, benchtop NMR was used to perform online monitoring of hydrolysis in real time by observing the solubilization of peptides from raw materials and the

subsequent increase in hydrolysate concentration.²³ Due to its relatively low cost and maintenance requirement, benchtop NMR has the potential to be deployed online at processing facilities. This work extends this method to include molecular sizing from high resolution diffusion ordered spectroscopy (HR-DOSY). These two measurements can quantitatively follow hydrolysis in real time both through direct measurement of yield (total protein) and average protein size, allowing the operator to stop the enzymatic process when the desired size has been reached. This will enable better control of many important chemical and physical properties of the product, such as bioactivity, flavor, and emulsification ability. The average protein size can also be used to calculate a degree of hydrolysis (DH), which is commonly used to follow the hydrolysis progress and evaluate the enzymatic rates. In this work, we show that benchtop NMR can be used to monitor the reduction in average molecular size in real time during the hydrolysis process.

1.2 | NMR theory

1.2.1 | Diffusion measurements

Pulsed-field gradient NMR is an established method to measure the self-diffusion coefficients of molecules.²⁴ As translational velocity through a fluid is related to molecular size, the self-diffusion coefficient can be used to derive a molecule's molecular weight. The pulsed field gradient experiment is performed by collecting a free induction decay (FID) at increasing gradient encoding strengths to

create a two-dimensional data set, with time on one axis and gradient strength on the other. As the gradient strength increases, the NMR signal becomes more sensitive to the motion of the molecules. The signal attenuation due to diffusion in the applied gradients follows the Stejskal–Tanner equation²⁵:

$$S = S_0 e^{-D\gamma^2 \delta^2 g^2 \Delta'} \quad (1)$$

where S_0 is the signal observed in the absence of a gradient, D is the diffusion coefficient of the molecule the signal originates from, γ is the magneto-gyric ratio of the observed nucleus, δ is the gradient duration, g is the gradient amplitude, and Δ' is the diffusion time in the limit of a small gradient duration as compared with the separation of the gradient pulses. When the time dimension is Fourier transformed into a standard NMR spectrum and the gradient dimension is fit to one or more diffusion coefficients and amplitudes, a frequency-dependent diffusion coefficient map with spectrum on one axis and diffusion coefficient on the other is produced. This can then be used to associate a diffusion coefficient with a specific species within the sample such as the water, or the protein at the aliphatic or the aromatic region of the spectrum (Figure 1).

1.2.2 | Molecular sizing

The self-diffusion coefficient, D , of a molecule in a fluid is related to its hydrodynamic radius, R_H , by²⁶

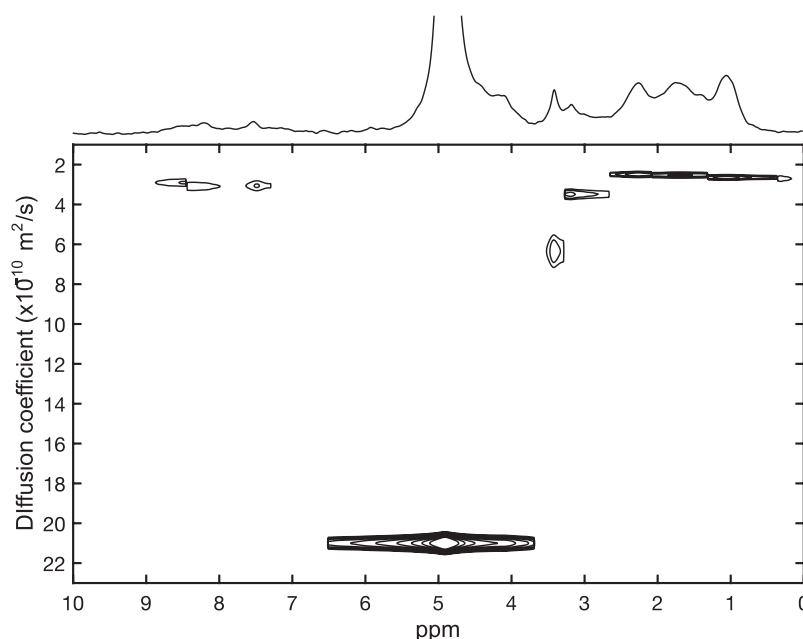


FIGURE 1 A typical two-dimensional DOSY map of hydrolysate with a 1D spectrum above.

$$D = \frac{k_B T}{6\pi\eta R_H} \quad (2)$$

where k_B is the Boltzmann constant, T is temperature, and η is the viscosity of the solvent. The hydrodynamic radius is related to molecular weight, M , through the scaling law

$$R_H \propto M^\nu \quad (3)$$

where ν is the Flory exponent dependent on the solvent quality and space filling properties of the molecule. The molecular weight and peptide length can then be estimated through this relationship. The scaling factor can be determined from a set of calibration standards and fitting to the equation:

$$\ln(D) = -\nu \ln(M) + C \quad (4)$$

This requires that the viscosity and temperature remain the same for each experiment.

Alternatively, for small molecules, a molecular weight can be estimated by making assumptions regarding the Stokes–Einstein equation.²⁷ This method is designed for small molecules that are densely packed and under 1.5 kDa. Of the 12 calibrations proteins used in this study, only 5 of them meet this requirement. Another method for controlling for the effect of viscosity and temperature during measurements is to include a calibration standard such as dioxane.¹⁶

The radius of hydration has been measured for many proteins,¹⁷ and the radius of gyration has been calculated from structures found in the Protein Database for even more.^{18,28} These predict a scaling factor with peptide length of 0.39 for proteins between 311 and 11,448 amino acids. This only covers the range of lysozyme to albumin in this work, and this is for proteins in a compact folded state, so this is not completely applicable. For peptide and proteins in a highly denatured state, that scaling factor increases to 0.58.¹⁶ This is the other extreme where the protein has been highly solubilized.

Peptides within hydrolysates are very likely to contain inflated radii of hydration relative to the compact sphere assumed by the Stokes–Einstein equation due to the peptide fragments being highly soluble, but these radii are likely to be well below that of highly denatured proteins. Therefore, the calibration samples, which are a mixture of proteins and peptides, will only roughly represent average molecular weight of the sample. This issue will equally impact calibration of SEC as it will NMR calibration. A series of representative peptide fragments would provide a more precise calibration curve. However, even a semiquantitative characterization hydrolysate has

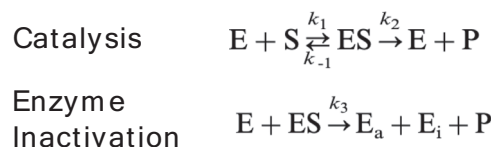
already been found useful. Therefore, by using these known shortcomings in the evaluation of sizing data, the analyst is able to put limitations on possible size range during measurement design.

1.2.3 | Degree of hydrolysis

The molecular weight distribution of protein hydrolysis sample is correlated to the degree of hydrolysis, which is the percentage of peptide bonds hydrolyzed, and can thus be used to estimate DH by

$$DH \approx \frac{\bar{m}_{aa}}{\bar{m}_h} \times 100\% \quad (5)$$

where \bar{m}_{aa} is the mean molecular weight of an amino acid in the starting protein and \bar{m}_h is the mean molecular weight of the peptides in the hydrolysate. While the DH is not necessary to characterize the products, it is a commonly used way to describe the progress of an enzymatic hydrolysis reaction in absence of information on molecular size. Calculating it allows for comparison of our diffusion NMR results with other analysis methods and provides a quantitative state of the reaction that can be used to evaluate the enzyme kinetics of the hydrolysis reaction. The enzyme kinetics were analyzed using a model proposed by Márquez and Vázquez²⁹ for the hydrolysis of hemoglobin by Alcalase



where it is assumed that the substrate concentration, S , is equal to the initial substrate concentration, S_0 , and is much greater than the Michaelis–Menton constant, K_M , catalysis, k_2 , is a zero-order reaction, and enzyme inactivation, k_3 , follows a second order rate. The degree of hydrolysis, DH , as a function of time, t , follows the equation:

$$DH = \frac{1}{b} \ln(1 + abt) \quad (6a)$$

where

$$a = \frac{k_2 E_0}{S_0}; \quad b = \frac{k_3 K_M}{k_2}. \quad (6b)$$

In this work, we evaluate using benchtop diffusion NMR spectroscopy as a potential method for following

hydrolysis reactions in order to control or optimize the process for industrial use. Signal from large proteins in solid material, such as tissue, relaxes very quickly and will not be measured by the techniques used here. Therefore, we measure only on the protein in solution that has been solubilized by the hydrolysis process or was created during sample preparation. The rate of change in protein weight will be dependent on the current size of the protein and how susceptible it is to further hydrolysis, among other enzyme kinetics rate determinants. This suggests that the NMR signal intensity will provide the overall yield of the hydrolysis and the diffusion derived molecular weight will characterize the protein size. In this work, while we have not controlled or optimized hydrolysis in real time from the NMR data, similar examples have been published for chemical reaction systems.³⁰ We believe the key step for on-the-fly control of hydrolysis is good information feedback from the NMR methods developed here. Although this study performed measurements at-line, the process could easily be performed online as well.

2 | MATERIALS AND METHODS

2.1 | Calibration samples

Two types of calibration samples were used in this study. First, commercial protein and peptide standards were purchased from Sigma Aldrich. The commercial standards provide a test case for DOSY NMR over a wide range of molecular weights (Table 1).

Second, a set of calibration samples were created by enzymatic hydrolysis of poultry. Four types of raw

materials and three types of enzymes were used to create a set of 12 hydrolysis products. Enzymatic hydrolysis was performed on the materials at 50°C for 80 min, and then the reaction ended by thermal inactivation of the enzymes. Average molecular weight of the hydrolysis products was obtained by SEC analysis. More information on sample creation and characterization can be found in the Materials and Methods section of Lindberg et al.³¹ Table 2 contains information on the raw material and molecular weight. The poultry hydrolysis products were used to test the ability of DOSY NMR to distinguish molecules more similar in molecular weight.

2.2 | Enzymatic hydrolysis

Enzymatic hydrolysis was performed on red cod (*Pseudophycis bachus*) samples obtained from a commercial vendor. Water was added to red cod fillet in a ratio of 3 to 1, homogenized in a blender, and then transferred to a reaction vessel and heated to 50°C. Alcalase 2.4 L (Novozymes, Denmark) was added to initiate the hydrolysis at a 0.15% by weight of the fish protein. The reaction was allowed to continue for 2 h and then was terminated by heating the sample to 90°C. Hydrolysate samples for NMR analysis were transferred from the reaction vessel to a 5-mm NMR tube and data was collected immediately without deactivating the enzymes. Because of the small sample volume (~400 µl), the hydrolysate samples cooled almost immediately to ambient temperature once decanted and temperature could be assumed to be stable during NMR measurement. Although enzymes were not deactivated, once the sample temperature has dropped to

TABLE 1 Calibration samples and molecular weights.

Sample	Molecular weight (g/mol)
Tryptophan HCl	204
Val-Tyr-Val	379
[D-Ala2]-leucine enkephalin (N/A)	570
Bradykinin fragment 1-7	757
Angiotensin II human	1046
Renin substrate tetradecapeptide porcine	1759
Insulin chain B oxidized from bovine pancreas	3496
Aprotinin from bovine lung	6511
Lysozyme	14,300
Carbonic anhydrase	29,000
Albumin from chicken egg white	44,287

TABLE 2 Calibration samples and average molecular weights.

Raw material	Enzyme	Molecular weight (g/mol)
Chicken carcass	Alcalase	1742.7
Chicken carcass	Corolase 2Ts	1902.4
Chicken carcass	Flavorzyme	1139.7
Mechanically deboned chicken	Alcalase	1502.4
Mechanically deboned chicken	Corolase 2Ts	2030.3
Mechanically deboned chicken	Flavorzyme	1404.3
Turkey carcass	Alcalase	1572.7
Turkey carcass	Corolase 2Ts	2016.6
Turkey carcass	Flavorzyme	1310.0
Mechanically deboned turkey	Alcalase	1599.8
Mechanically deboned turkey	Coralase 2Ts	1829.2
Mechanically deboned turkey	Flavorzyme	1380.7

approximately 25°C, the reaction rate is slowed significantly.

2.3 | NMR data acquisition

2.3.1 | Calibration samples

Calibration samples were dissolved in deionized water at concentrations ranging from 1.7–50 mg/ml depending on sample availability and solubility except for Val-Tyr-Val, which was dissolved in 5% trifluoroacetate. NMR data of the calibration samples were collected using the BPP-LED NMR sequence³² on both benchtop (Magritek, 43 MHz) and high-field (Jeol 500 MHz) systems. Due to the large range in molecular weights, a range of NMR acquisition parameters were needed in order to adequately measure the anticipated diffusion coefficients of different samples. These are shown in Table 3 as well as described as follows: for the bench top NMR, this required a gradient pulse ranging in duration from 1.75 to 5 ms, a diffusion time from 60 to 200 ms, a LED delay of 20 ms, and a maximum gradient strength varying from 300 to 650 mT/m. There were 16 to 128 averages required to obtain adequate signal to noise depending on sample concentration. For the high-field system, the maximum gradient was 300 mT/m, gradient duration varied from 2.5 to 5 ms, diffusion delay ranged from 100 to 200 ms, and LED delay was between 20 and 50 ms. The NMR signal at high field was averaged for 16 to 64 scans. Diffusion is sensitive to temperature, so samples were equilibrated in the benchtop system prior to measurement at 27°C. The measurements in the high-field system were done at ambient temperature of 21°C.

2.3.2 | Reaction monitoring

NMR data were collected using a modified pulsed field gradient stimulated echo sequences called Oneshot45³³

TABLE 3 NMR acquisition parameters.

Parameter	Benchtop NMR	High-field NMR
Frequency (MHz)	43	500
Gradient pulse duration (ms)	1.75–5	2.5–5
Diffusion time (ms)	60–200	100–200
LED delay (ms)	20	20–50
Maximum gradient amplitude (T/m)	0.30–0.65	0.3
Averages	16–128	16–64

Abbreviation: NMR, nuclear magnetic resonance.

using a maximum gradient of 0.75 T/m, a 3-ms trapezoidal gradient pulse, and a diffusion time of 50 ms. Nine gradient steps were collected, and the first one was discarded due to excessive water signal overlapping with the peaks of interest and distorting the baseline. The total NMR experiment time was 3 min 36 s (16 scans, 1.5-s cycle time). The spectrum from the second gradient step (287 mT m⁻¹) was extracted (Figure 1) from each hydrolysis time point to follow the reaction process using spectroscopy. The Oneshot45 sequence reduces the minimum scans needed for phase cycling and allows for better time resolution.

2.4 | Hydrolysis diffusion processing procedures

An HR-DOSY contour map was created for each hydrolysis time point using General NMR Analysis Toolbox (GNAT)³⁴ in Matlab (Mathworks), Figure 1. The spectra were manually zero-order phase corrected, and then 3 Hz of line broadening and a second-order baseline correction were applied. Diffusion coefficients were determined from the fit of peak heights at 0.95 and 2.15 ppm to Equation (1), which were subsequently averaged together to give a single value with reduced scatter.

3 | RESULTS

3.1 | Calibration of molecular weight

We confirmed that using DOSY NMR produced accurate calculated molecular weights by two methods. The first used a range of pure proteins of known molecular weights. The second used hydrolysates with different molecular weight distributions characterized by gel filtration chromatography.

3.1.1 | Protein and peptide standards

The protein and peptide standards were measured on both benchtop and high-field NMR system. Some samples were of so low concentration such that only the high-field data were able to measure a diffusion coefficient. The diffusion coefficients were used to predict molecular weight using the Stokes–Einstein Gierer–Wirtz estimation²⁷ and plotted against the actual molecular weight in Figure 2a. This shows that diffusion coefficients can be used to reliably predict molecular weight of proteins and peptides over a range applicable to protein hydrolysates and monitoring the hydrolysis process.

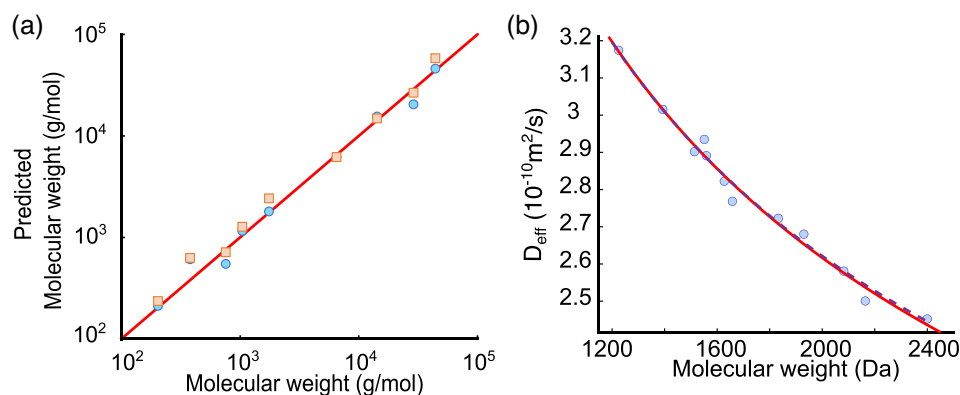


FIGURE 2 (a) Calibration of diffusion coefficient and molecular weight with protein and peptide standards, where blue circles are measurements made on the benchtop NMR instrument and orange squares represent measurement on a 500 MHz high-field nuclear magnetic resonance system. (b) Mean weight of the characterized poultry hydrolysates scale with the benchtop NMR diffusion measurement by the Flory scaling law (fit).

3.1.2 | Characterized poultry hydrolysates

The hydrolysate is a complex mixture of protein chains and small molecules such as amino acids. These have overlapping or superimposed NMR signals that do not fit standard models for predicting molecular weight from the diffusion coefficient. We, therefore, empirically derive a scaling relationship from a calibration curve of characterized protein hydrolysates, which had a Flory exponent of 0.39. The poultry hydrolysates had an average molecular weight ranging from approximately 1200 to 2400 g/mol (Figure 2b). The peak amplitude at 2.1 ppm was used to determine the diffusion coefficients because there was a systematic error observed with certain samples at 0.9 ppm. This error is speculated to be due to differing fat content of some samples. The resulting equation was then used to calculate the average molecular weight of the fish hydrolysates from their diffusion coefficients. Even though these hydrolysates are complicated samples, they match the expected diffusion coefficients for single molecules of the same molecular weights at 27°C and a viscosity 2% greater than water, shown by a red fit line in Figure 2b.²⁷

3.2 | Monitoring hydrolysate physical parameters

Once confidence was established in the technique using the reference samples, the method was applied to samples undergoing enzymatic hydrolysis. The measured diffusion coefficients increased during the EPH, showing a general trend of protein being broken down into smaller components that diffuse faster (Figure 3a). This indicates a decrease in hydrodynamic radius of the solubilized

protein molecules, which would be expected for proteins undergoing hydrolysis. The molecular weights were calculated using the calibration curve created from the poultry hydrolysates (Figure 3b). The peptides' weights consistently decreased and stabilized at about 2000 g/mol after 60 min. Molecular weights were used to calculate the degree of hydrolysis, which is a standard measure of progress of enzymatic hydrolysis. The degree of hydrolysis approached a maximum of 6% over the 2-h reaction (Figure 3c). The integral of the aliphatic protons between 0.75 and 1.25 ppm is shown in Figure 3d. The integrals were normalized by dividing by their standard deviation so that they could be compared with PCA analysis and previous work.^{35,36} This shows that the solubilization of protein and peptides in the hydrolysate increases rapidly and then stabilizes over the course of the reaction. PCA analysis was also performed on the spectral region between 0 and 2.75 ppm. The scores of the first component follow the same trend as the integrals are also plotted in Figure 3d. As there tends to be significant change in the sample composition prior to the start of hydrolysis and just after, therefore, no zero-time point is included in the data except the degree of hydrolysis and the normalized PCA where at time zero DH is also zero.

The hydrolysis data was fit to the enzyme kinetics model (Equation 6a). The rate a was 0.36 min⁻¹ for the degree of hydrolysis data and 2.0 min⁻¹ for the integrals and the scores of the first principal component. The enzyme kinetic rate (Table 4) was calculated from degree of hydrolysis data and Equation (6b), where E_0 was 0.75 AU and S_0 was estimated to be 25% of the weight of the fillet (46.25 g, water being the balance of the weight). The enzymatic rate, k_2 , was calculated to be 22 g AU⁻¹ min⁻¹ (95% confidence interval [14, 31]). The enzymatic rate cannot be calculated from the integral

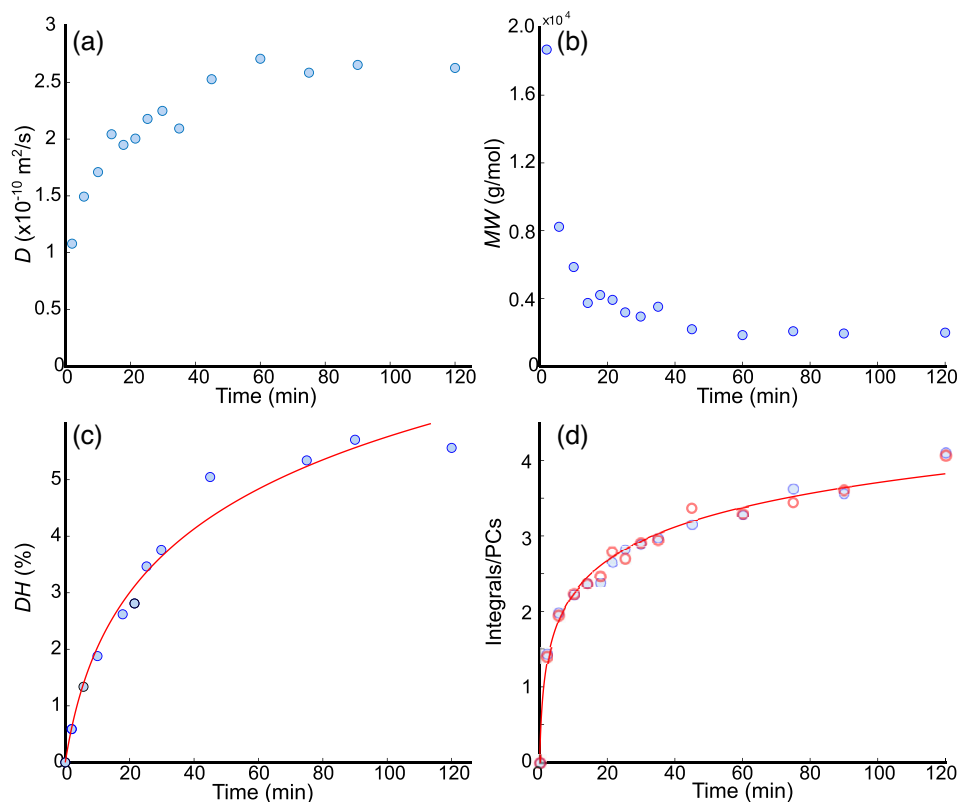


FIGURE 3 (a) Diffusion, (b) molecular weight, (c) degree of hydrolysis, and (d) integral amplitude (blue dots) and principal components normalized by standard deviation (σ) (red circles) plotted against time since initiating the hydrolysis.

TABLE 4 Hydrolysis rate and R^2 of fits to integral amplitudes, scores, and degree of hydrolysis.

Monitoring method	Enzyme kinetics		
	a (min^{-1})	b	i^2
Spectrum integral	2.0 (± 0.4)	1.5 (± 0.09)	0.987
Scores (PC1)	2.0 (± 0.4)	1.5 (± 0.09)	0.985
Degree of hydrolysis	0.36 (± 0.006)	0.5 (± 0.06)	0.974

data due to the units not actually being degree of hydrolysis.

4 | DISCUSSION

The results show the potential of NMR benchtop spectroscopy for online monitoring of enzymatic hydrolysis. The protein concentration can be derived from the NMR signal intensity and the mean peptide size from the mean self-diffusion coefficient of the hydrolysate. Both properties were able to be monitored at a rate that was fast enough such that they could be used to steer decision making about the hydrolysis process. One surprising result was how well the rates of protein concentration and molecular size tracked each other. It appears that for red cod fillet, the solubilization and the further hydrolysis of these peptides occurs at a similar rate. In the previous

study where the protein concentration alone was monitored by benchtop NMR spectroscopy,²³ the reaction appeared to proceed more rapidly compared with rates for similar reactions reported in the literature. This was interpreted as the measurement could quantify the amount of protein solubilized, but the further breakdown of the proteins by the enzymes could not be captured by the method. This meant that the measurement would observe an initial burst of solubilization that did not represent the hydrolysis reaction properly. In this work, that initial burst is observed by a steeper initial rise in integral amplitude compared with the initial rise in degree of hydrolysis. Because the measurements were performed inline on samples that had cooled, the sample could be assumed to be roughly at equilibrium. However, for online NMR measurements, the sample will continue to evolve during measurement, affecting results made with a standard DOSY sequence. Therefore, a technique p-DOSY, which is optimized for out-of-equilibrium systems, should be used in this situation.

Although there is a high correlation (0.88) between degree of hydrolysis and signal intensity, as shown in Figure 4a, this is coincidental. Once the protein is solubilized, the integral will be relatively independent of the number of peptide bonds in the peptide change. A given mass of small peptides will produce the same integral as the same mass of larger peptides and protein fragments. As such, while the rates from concentration and self-

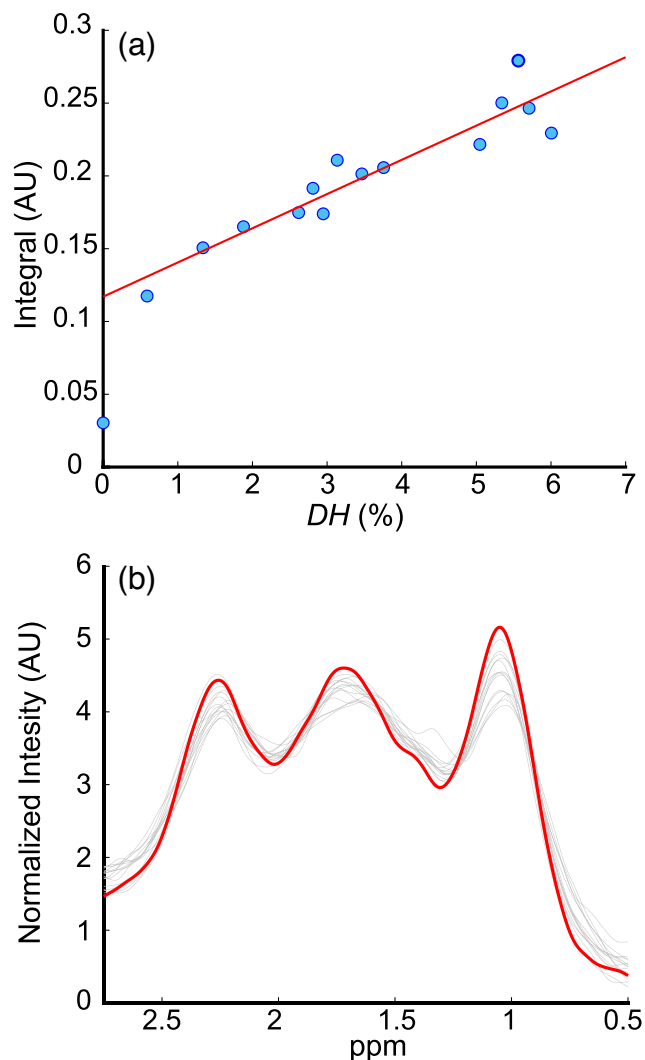


FIGURE 4 (a) the correlation of integral intensity with degree of hydrolysis determined from diffusion coefficient of the hydrolysate. (b) Spectra collected in the second gradient step of each time point (gray) and first component of principal component analysis of the spectra (red).

diffusion follow a similar arc, their final values will have different meanings and one cannot necessarily be derived from the other. We believe the high correlation here may come from the choice of source material. While the red cod fillets contained some skin and cartilage, they consisted of mostly easy to digest muscle. This will not necessarily be the case for all raw materials, such as one that is more difficult to hydrolyze with high percentages of cartilage and bone or proteins that are less soluble until considerably hydrolyzed, such as casein. Furthermore, using protein concentration as an indicator of reaction process will fail in a continuous reactor, where protein concentrations could be more or less constant or even erratic. The diffusion coefficient, on the other hand, is independent of sample concentration and pH and therefore can

complement intensity dependent concentration monitoring measurements.

Hydrolysis was previously monitored by high-field NMR³⁵ and FT-IR¹³ spectroscopies using multivariate models. In order to compare different methods, principal component analysis (PCA) has been used to normalize the data.³⁵ We compared simple integration of the NMR spectral region used in our analysis to the scores of the first principal component (PC1) for the aliphatic region (0–2.75 ppm) and found a correlation of 0.999.²³ However, the correlation of the integral and therefore first component to the degree of hydrolysis is only 0.88 (Figure 4a). The first component is plotted on the normalized spectra collected during the hydrolysis, excluding the zero time-point that is an outlier (Figure 4b). The main variation in the spectra over the hydrolysis, which is described by the principal component, mirrors the spectrum and supports the theory that the PCA only follows an increase in spectral intensity. This is also observed in Sundekilde et al.³⁶ where the only negative peaks in the first component arise from protons that are sensitive to the pH change during the hydrolysis. NMR signal is linear with concentration; therefore, the scores are indicative of protein concentration, and in the context of hydrolysis, they are describing the solubilization of the protein. Therefore, there seems to be little advantage to developing a PCA model over simple integration of the relevant areas of the spectrum.

In addition to its speed and noninvasive nature, one of the biggest advantages of using DOSY to monitor enzymatic hydrolysis is that it gives a direct measure of average protein size. Degree of hydrolysis is a relative measure that is very useful for describing the enzyme kinetics; however, it does not describe the product. Protein size influences functional attributes of the hydrolysate such as flavor and foaming quality, while degree of hydrolysis is less indicative and protein concentration possibly even less. It was noted that the calculated degree of hydrolysis was lower than many other examples in the literature.^{37–39} We believe this arises from the fact that the measurement will only see solubilized protein. Protein that is not in solution at the start of measurement or is very large will not be included in the initial estimate of molecular weight. Therefore, this technique needs to be treated with caution when comparing it to other methods to calculate degree of hydrolysis.

While we only tested the system on a lean fish, we expect the method should be applicable to many other types of common hydrolysis feed stocks, including fatty materials such as salmon by-products. In previous work, we showed that although enzymatic hydrolysis of a fatty fish like salmon will produce oil, the aromatic region of the spectrum could be used to monitor the hydrolysis.²³

It is likely that a different calibration would be needed to compensate for the amide protons in this area of the spectrum that might increase the apparent diffusion coefficient due to chemical exchange with water. Although DOSY NMR measurements are less sensitive to variations in sample composition than techniques based on multivariate models, sample inhomogeneity will still have an influence on the results. Therefore, for at-line measurements, ensuring the measured sample is representative of the main batch will be important to produce reliable results and reduce scatter.

In summary, benchtop NMR spectroscopy has both the speed and sensitivity necessary to be applied for real-time monitoring, enabling rapid feedback and control of the hydrolysis process. By developing a technique that can continuously assess protein size, adjustments can be made in real-time to optimize enzyme dosage, reaction time, temperature, or pH, leading to improved efficiency and yield. This dynamic control would allow for on-the-fly optimization, minimizing the need for lengthy trial-and-error experiments and aiding in designing specific hydrolysis strategies to generate peptides with desired bioactivity, solubility, or sensory characteristics.

5 | CONCLUSIONS

NMR benchtop spectroscopy shows the capacity to be used for real-time monitoring of enzymatic hydrolysis. The DOSY measurement has an advantage over other types of methods because it provides the molecular weight of the hydrolysate. The method also gives a measure of solubilized protein concentration and average protein size in addition to an estimate of degree of hydrolysis. Because of the ability to separate hydrolysate constituents by both spectroscopy and diffusion, the method is expected to be applicable to monitoring enzymatic hydrolysis of many types of feedstocks.

ACKNOWLEDGMENTS

The authors thank Mabit for their financial support (UB0071) and Novozymes for the enzymes. The authors thank Ian Vorster, Diana Lindberg, Runar Gjerp Solstad, Birthe Vang, and Sileshi Wubshet for helpful discussions.

PEER REVIEW

The peer review history for this article is available at <https://www.webofscience.com/api/gateway/wos/peer-review/10.1002/mrc.5427>.

ORCID

Evan R. McCarney  <https://orcid.org/0000-0002-4921-7580>

REFERENCES

- [1] T. Rustad, I. Storror, R. Slizyte, *Int. J. Food Sci. Technol.* **2011**, *46*, 2001. <https://doi.org/10.1111/j.1365-2621.2011.02736.x>
- [2] F. Shahidi, *Maximising the Value of Marine By-products*, Woodhead Publishing **2006**. Sawston, United Kingdom.
- [3] H. G. Kristinsson, B. A. Rasco, *Crit. Rev. Food Sci. Nutr.* **2000**, *40*, 43. <https://doi.org/10.1080/10408690091189266>
- [4] S. Sathivel, S. Smiley, W. Prinyawiwatkul, P. Bechtel, *J. Food Sci.* **2005**, *70*, 401. <https://doi.org/10.1111/j.1365-2621.2005.tb11437.x>
- [5] R. SilzYTE, R. Mozuraityte, O. Martinez-Alvarez, E. Falch, M. Fouchereau-Peron, T. Rustad, *Process Biochem.* **2009**, *44*, 668. <https://doi.org/10.1016/j.procbio.2009.02.010>
- [6] T. Aspevik, Å. Oterhals, S. Rønning, T. Altintzoglou, S. Wubshet, A. Gildberg, N. Afseth, R. Whitaker, D. Lindberg, *Top. Curr. Chem.* **2017**, *53*, 375. <https://doi.org/10.1007/s41061-017-0143-6>
- [7] M. Abdollahi, I. Undeland, *Food Bioproc. Tech.* **2018**, *11*, 1733. <https://doi.org/10.1007/s11947-018-2138-x>
- [8] S. Eriksen, *Biochem. Soc. Trans.* **1982**, *10*, 285. <https://doi.org/10.1042/bst0100285>
- [9] M. I. Mahmoud, W. T. Malone, C. T. Cordle, *J. Food Sci.* **1992**, *57*, 1223. <https://doi.org/10.1111/j.1365-2621.1992.tb11304>
- [10] N. T. Hoyle, J. H. Merritt, *J. Food Sci.* **1994**, *59*, 76. <https://doi.org/10.1111/j.1365-2621.1994.tb06901.x>
- [11] K. Maehashi, M. Matsuzaki, Y. Yamamoto, S. Udaka, *Biosci. Biotechnol. Biochem.* **1999**, *63*, 555. <https://doi.org/10.1271/bbb.63.555>
- [12] M. Ovissipour, A. Abedian, A. Motamedzadegan, B. Rasco, R. Safari, H. Shahiri, *Food Chem.* **2009**, *115*, 238. <https://doi.org/10.1016/j.foodchem.2008.12.013>
- [13] S. G. Wubshet, I. Måge, U. Böcker, D. Lindberg, S. H. Knutsen, A. Rieder, D. Rodriguez, N. K. Afseth, *Anal. Methods* **2017**, *9*, 4247. <https://doi.org/10.1039/c7ay00865a>
- [14] K. A. Kristoffersen, K. H. Liland, U. Bocker, S. G. Wubshet, D. Lindberg, S. J. Horn, N. K. Afseth, *Talanta* **2019**, *205*, 120084. <https://doi.org/10.1016/j.talanta.2019.06.084>
- [15] D. Berek, *J. Sep. Sci.* **2010**, *33*, 315. <https://doi.org/10.1002/jssc.200900709>
- [16] D. K. Wilkins, S. B. Grimshaw, V. Receveur, C. M. Dobson, J. A. Jones, L. J. Smith, *J. Biochem.* **1999**, *38*, 16424. <https://doi.org/10.1021/bi991765q>
- [17] S. Auge, P. O. Schmit, C. A. Crutchfield, M. T. Islam, D. J. Harris, E. Durand, M. Clemancey, A. A. Quoineaud, J. M. Lancelin, Y. Prigent, F. Taulelle, M. A. Delsuc, *J. Phys. Chem. B* **1914**, 2009, 113. <https://doi.org/10.1021/jp8094424>
- [18] M. B. Enright, D. M. Leitner, *Phys. Rev. E Stat. Nonlin. Soft Matter Phys.* **2005**, *71*, 011912. <https://doi.org/10.1103/PhysRevE.71.011912>
- [19] E. F. Dudas, A. Bodor, *Anal. Chem.* **2019**, *91*, 4929. <https://doi.org/10.1021/acs.analchem.8b05617>
- [20] B. Tang, K. Chong, W. Massefski, R. Evans, *J. Phys. Chem. B* **2022**, *126*, 5887. <https://doi.org/10.1021/acs.jpcc.2c03554>
- [21] C. L. Szabó, F. Sebák, A. Bodor, *Anal. Chem.* **2022**, *94*, 7885. <https://doi.org/10.1021/acs.analchem.2c00481>
- [22] R. D. Whitehead, C. M. Teschke, A. T. Alexandrescu, *Protein Sci.* **2022**, *31*, e4321. <https://doi.org/10.1002/pro.4321>
- [23] K. E. Anderssen, E. R. McCarney, *Food Contr.* **2019**, *112*, 107053. <https://doi.org/10.1016/j.foodcont.2019.107053>

- [24] P. T. Callaghan, *Translational Dynamics and Magnetic Resonance: Principles of Pulsed Gradient Spin Echo NMR*, Oxford University Press **2011**. Great Clarendon Street, Oxford OX2 6DP, United Kingdom.
- [25] E. O. Stejskal, J. E. Tanner, *J. Chem. Phys.* **1965**, *42*, 288. <https://doi.org/10.1063/1.1695690>
- [26] A. Einstein, *Ann. Phys.* **1905**, *322*, 549. <https://doi.org/10.1002/andp.19053220806>
- [27] R. Evans, G. Dal Poggetto, M. Nilsson, G. A. Morris, *Anal. Chem.* **2018**, *90*, 3987. <https://doi.org/10.1021/acs.analchem.7b05032>
- [28] R. Burioni, D. Cassi, F. Cecconi, A. Vulpiani, *Proteins* **2004**, *55*, 529. <https://doi.org/10.1002/prot.20072>
- [29] M. C. Márquez, M. A. Vázquez, *Process Biochem.* **1999**, *35*, 111. [https://doi.org/10.1016/s0032-9592\(99\)00041-2](https://doi.org/10.1016/s0032-9592(99)00041-2)
- [30] K. Meyer, S. Kern, N. Zientek, G. Guthausen, M. Maiwald, *TrAC Trends in Anal. Chem.* **2016**, *83*, 39. <https://doi.org/10.1016/j.trac.2016.03.016>
- [31] D. Lindberg, K. A. Kristoffersen, H. de Vogel-van den Bosch, S. G. Wubshet, U. Bocker, A. Rieder, E. Fricke, N. K. Afseth, *Process Biochem.* **2021**, *110*, 85. <https://doi.org/10.1016/j.procbio.2021.07.014>
- [32] C. S. Johnson Jr., *Prog. Nucl. Magn. Reson. Spectrosc.* **1999**, *34*, 203. [https://doi.org/10.1016/S0079-6565\(99\)00003-5](https://doi.org/10.1016/S0079-6565(99)00003-5)
- [33] A. Botana, J. A. Aguilar, M. Nilsson, G. A. Morris, *J. Magn. Reson.* **2011**, *208*, 270. <https://doi.org/10.1016/j.jmr.2010.11.012>
- [34] L. Castanar, G. D. Poggetto, A. A. Colbourne, G. A. Morris, M. Nilsson, *Magn. Reson. Chem.* **2018**, *56*, 546. <https://doi.org/10.1002/mrc.4717>
- [35] M. Bevilacqua, G. Pratico, J. Plesner, M. Molloy, T. Skov, F. H. Larsen, *Food Res. Int.* **2017**, *102*, 256. <https://doi.org/10.1016/j.foodres.2017.09.069>
- [36] U. K. Sundekilde, L. Jarno, N. Eggers, H. C. Bertram, *LWT* **2018**, *95*, 9. <https://doi.org/10.1016/j.lwt.2018.04.055>
- [37] F. Guerad, L. Duffose, D. De La Boise, A. Binet, *J. Mol. Catal. B: Enzym.* **2001**, *11*, 1051. [https://doi.org/10.1016/S1381-1177\(00\)00031-X](https://doi.org/10.1016/S1381-1177(00)00031-X)
- [38] G. A. Gbogouri, M. Linder, J. Fanni, M. Parmentier, *J. Food Sci.* **2006**, *29*, 615. <https://doi.org/10.1111/j.1365-2621.2004.tb09909.x>
- [39] T. Aspevik, H. Egede-Nissen, Å. Oterhals, *Food Technol. Biotechnol.* **2016**, *54*, 421. <https://doi.org/10.17113/ftb.54.04.16.4553>

How to cite this article: E. R. McCarney, K. A. Kristoffersen, K. E. Anderssen, *Magn Reson Chem* **2024**, *1*. <https://doi.org/10.1002/mrc.5427>